Synthesis of Superwide-Band Matching Adapters in Round Coaxial Lines

Boris Markovich Kats, Valery Petrovich Meschanov, and Alexander Lvovich Khvalin

***Abstract*—An algorithm for modeling stepped axially symmetrical discontinuities in round coaxial transmission lines (RCTLs) based on the numerical solution of an integral equation is proposed in this paper. The algorithm has been tested and the results of discontinuity parameter computations have been compared with those of the other researchers. High efficiency of the algorithm allowed us to realize the procedure of the numerical synthesis of the devices on RCTLs. The tabulated and graphical results of the synthesis of superwide-band adapters for 50-Ω-to-50-Ω RCTLs with air medium are presented. The coaxial adapter for the line of 2.4/1.042 mm in cross section to that of 7.0/3.04 mm has been tested over the frequency range from dc to 50 GHz.**

***Index Terms*—Adapter, coaxial lines, electrodynamics, field matching, integral equations, synthesis.**

I. Introduction

Stepped axially symmetrical variations of geometrical dimensions constitute the most widely spread type of discontinuities in round coaxial transmission line (RCTLs) (Fig. 1). Many publications [1]–[6] have been devoted to their analysis. The methods currently used and the program packages of their electrodynamics modeling are in the majority of cases based on universal finite-difference circuits or finite-element ones. The price for their universality is their high algorithm complexity, which requires the use of highly productive computers and actually excludes the possibility of direct numerical synthesis of the devices on RCTLs.

This paper describes the algorithm for electrodynamics modeling of stepped axially symmetrical discontinuities in RCTLs. The algorithm is based on solving the integral equation obtained with the application of the field-matching method. The method of moments has been used for numerical solution of the integral equation. High numerical efficiency of the algorithm allowed us to realize the program of the direct numerical synthesis of individual types of the devices on RCTLs.

The results of the synthesis of matched stepped adapters for RCTLs with large difference between the geometric dimensions and the data of experimental research over the frequencies up to 50 GHz are presented here.

II. Mathematical Model of Discontinuity

Let us consider the process of TEM-wave propagation in the coaxial line with stepped variation of radii a_i, b_i of the inner and outer conductors [see Fig. 1(a) and (b)]. To model the system, we will apply the method of integral equations. Let us consider its idea on the example of a simple electrodynamic system with a single discontinuity [see Fig. 1(a)]. Let us assume that, in the inlet transmission lines, there exists single-mode power propagation. The fields in areas I and II [see Fig. 1(a)] are presented in the form of incident and reflected eigenwaves

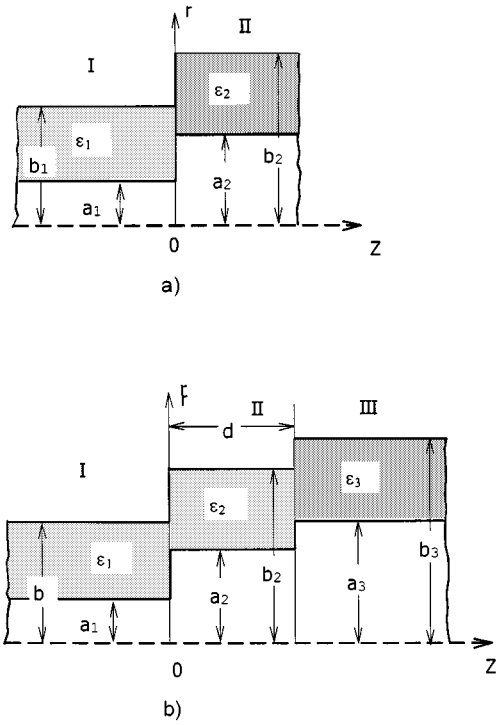

Fig. 1. Stepped axially symmetrical discontinuities. (a) Single. (b) Double.

of RCTLs. We also take into account the fact that due to azimuth symmetry, only E_{0n} waves are being excited in the area of discontinuities. Thus, in area I, we have

$$E_r^{\mathrm{I}} = \left(\exp\left(-ik_0 z\sqrt{\varepsilon_1}\right) - \Gamma_0 \exp\left(ik_0 z\sqrt{\varepsilon_1}\right)\right)\Big/ r - \sum_{n=1}^{\infty} \Gamma_n \alpha_n Z_1^{\mathrm{I}}(\chi_n r)\exp(\alpha_n z)\Big/ \chi_n$$

$$H_\varphi^{\mathrm{I}} = \left(\exp\left(-ik_0 z\sqrt{\varepsilon_1}\right) + \Gamma_0 \exp\left(ik_0 z\sqrt{\varepsilon_1}\right)\right)\omega\sqrt{\varepsilon_1}\Big/(rk_0) + i\omega\varepsilon_1 \sum_{n=1}^{\infty} \Gamma_n Z_1^{\mathrm{I}}(\chi_n r)\exp(\alpha_n z)\Big/\chi_n \quad (1)$$

and in area II, we have

$$E_r^{\mathrm{II}} = T_0 \exp\left(-ik_0 z\sqrt{\varepsilon_2}\right)\Big/ r - \sum_{m=1}^{\infty} T_m \beta_m Z_1^{\mathrm{II}}(\kappa_m r)\cdot\exp(-\beta_m z)\Big/\kappa_m$$

$$H_\varphi^{\mathrm{II}} = T_0 \exp\left(-ik_0 z\sqrt{\varepsilon_2}\right)\omega\sqrt{\varepsilon_2}\Big/(rk_0) - i\omega\varepsilon_2 \sum_{m=1}^{\infty} T_m Z_1^{\mathrm{II}} \cdot(\kappa_m r)\exp(-\beta_m z)\Big/\kappa_m \quad (2)$$

where $\alpha_n = \sqrt{\chi_n^2 - \varepsilon_1 k_0^2}$, $\beta_m = \sqrt{\kappa_m^2 - \varepsilon_2 k_0^2}$, and $k_0 = 2\pi/\lambda$. In the above expressions, $Z_1^{\mathrm{I}}(\chi_n r)$, $Z_1^{\mathrm{II}}(\kappa_m r)$ are the eigenfunctions of areas I and II

$$Z_1^{\mathrm{I}}(\chi r) = J_1(\chi r)N_0(\chi b_1) - J_0(\chi b_1)N_1(\chi r)$$
$$Z_1^{\mathrm{II}}(\kappa r) = J_1(\kappa r)N_0(\kappa b_2) - J_0(\kappa b_2)N_1(\kappa r)$$

Manuscript received June 16, 2000.

The authors are with the Central Institute of Measuring Equipment, Saratov 410090, Russia.

Publisher Item Identifier S 0018-9480(01)01700-8.

χ and κ are the roots of transcendental equations

$$J_0(\chi a_1)N_0(\chi b_1) = J_0(\chi b_1)N_0(\chi a_1)$$
$$J_0(\kappa a_2)N_0(\kappa b_2) = J_0(\kappa b_2)N_0(\kappa a_2)$$

J_0 denotes Bessel's functions of the first kind, N_0 denotes Bessel's functions of the second kind, and Γ_n, T_m are, respectively, the reflection and transmission coefficients for the main ($n = 0$) and higher ($n > 1$) E_{0n} waves. The component E_r of the electric field in the plane $z = 0$ will be denoted by $E(r)$. With $z = 0$, we obtain from (1) and (2)

$$(1-\Gamma_0)\Big/ r - \sum_{n=1}^{\infty} \Gamma_n \alpha_n Z_1^{\mathrm{I}}(\chi_n r)\Big/ \chi_n = E(r)$$
$$T_0 \Big/ r - \sum_{m=1}^{\infty} T_m \beta_m Z_1^{\mathrm{II}}(\kappa_m r)\Big/ \kappa_m = E(r). \tag{3}$$

The boundary conditions in the plane $z = 0$ have the form

$$H_\varphi^{\mathrm{I}} = H_\varphi^{\mathrm{II}}, \qquad P_1 < r < P_2$$
$$E_r^{\mathrm{I}},\ E_r^{\mathrm{II}} = 0, \qquad a_1 < r < a_2,\ b_1 < r < b_2 \tag{4}$$

where $P_1 = \max(a_1, a_2)$; $P_2 = \min(b_1, b_2)$. Using the orthogonality of Bessel's functions and the boundary conditions (4), we get

$$\Gamma_0 = 1 - 1 \Big/ \ln(b_1/a_1) \int_{P_1}^{P_2} E(r)\, dr$$
$$\Gamma_n = -\chi_n \Big/ (\alpha_n S_{1n}) \int_{P_1}^{P_2} E(r) Z_1^{\mathrm{I}}(\chi_n r) r\, dr$$
$$T_0 = 1 \Big/ \ln(b_2/a_2) \int_{P_1}^{P_2} E(r)\, dr$$
$$T_m = -\kappa_m \Big/ (\beta_m S_{2m}) \int_{P_1}^{P_2} E(r) Z_1^{\mathrm{II}}(\kappa_m r) r\, dr \tag{5}$$

where the integration is over the "clearance" of the waveguides $[P_1, P_2]$. The factors S_{1n}, S_{2n} in (5) are defined as follows:

$$S_{1n} = 0.5\Big(b_1^2\Big(Z_1^{\mathrm{I}}(\chi_n b_1)\Big)^2 - a_1^2\Big(\Big(Z_1^{\mathrm{I}}(\chi_n a_1)\Big)^2 - Z_0^{\mathrm{I}}(\chi_n a_1) Z_2^{\mathrm{I}}(\chi_n a_1)\Big)\Big)$$
$$S_{2m} = 0.5\Big(b_2^2\Big(Z_1^{\mathrm{II}}(\kappa_m b_2)\Big)^2 - a_2^2\Big(\Big(Z_1^{\mathrm{II}}(\kappa_m a_2)\Big)^2 - Z_0^{\mathrm{II}}(\kappa_m a_2) Z_2^{\mathrm{II}}(\kappa_m a_2)\Big)\Big). \tag{6}$$

In (6), it is implied that

$$Z_o^{\mathrm{I}}(\chi_n r) = J_i(\chi_n r)N_0(\chi_n b_1) - J_0(\chi_n b_1)N_i(\chi_n r)$$
$$Z_i^{\mathrm{II}}(\kappa_m r) = J_i(\kappa_m r)N_0(\kappa_m b_2) - J_0(\kappa_m b_2)N_i(\kappa_m r).$$

With the condition (4) for magnetic fields, after having performed elementary transformations, we get the integral equation

$$2\sqrt{\varepsilon_1} - \int_{P_1}^{P_2} E(r)\, dr \Big(\sqrt{\varepsilon_1}/\ln(b_1/a_1) + \sqrt{\varepsilon_2}/\ln(b_2/a_2)\Big) - ik_0 r \Bigg(\varepsilon_1 \sum_{n=1}^{\infty} \int_{P_1}^{P_2} rE(r) Z_1^{\mathrm{I}}(\chi_n r)\, dr\, Z_1^{\mathrm{I}}(\chi_n r) \Big/ (\alpha_n S_{1n}) + \varepsilon_2 \sum_{m=1}^{\infty} \int_{P_1}^{P_2} rE(r) Z_1^{\mathrm{II}}(\kappa_m r)\, dr\, Z_1^{\mathrm{II}}(\kappa_m r) \Big/ (\beta_m S_{2m})\Bigg) = 0. \tag{7}$$

Thus, the problem of analysis reduces to the solution of integral equation (7).

The existence of several discontinuities is possible in the devices on RCTLs. In case such discontinuities are arranged so that the extreme fields of the neighbor discontinuities are not in superposition, they may be regarded as single ones and interacting only on the main mode. A single-wave method of circuit theory can be used for the computation of the electrical parameters of such electrodynamic systems. In a more general case, the diffraction result will be defined by the interaction of discontinuities on higher modes as well. In practice, the most important case is the system of two discontinuities [see Fig. 1(b)]. The approach described above may be applied for the computation of such systems. After the tangential components of the fields at the boundaries of uniform areas I–III have been matched by analogy with (7), the system of two integral equations for the functions of the tangential components of the electric-field strength at the two boundaries of the separation of the above areas is obtained. Being cumbersome, the corresponding expressions are omitted here.

III. Numerical Realization

Let us apply the method of moments in order to solve the integral equations of type (7) [2]–[5]. The representation of the unknown function $E(r)$ in the form of a set according to the system of linearly independent functions

$$E(r) = \sum_{j=1}^{\infty} U_j f_j(r) \tag{8}$$

results in the transformation of the equation of type (7) to the system of linear equations in the unknown coefficients U_j. This system can be solved numerically after having been reduced by specifying the final term number N in the expansion (8) and the final term number in the expansion of the Green's function. The main problem while computing the matrix coefficients of the system of linear equations is the computation of the integrals

$$\int_{P_1}^{P_2} f_j(r) r Z_1(cr)\, dr \tag{9}$$

since, in case of a poor choice of the f_j-function system, the time consumption will be large.

The numerical experiments performed by the authors define the set of the basic functions of the form $1/r$ as an optimum one for modeling the electrodynamics systems under consideration. In view of this, let us represent the unknown function $E(r)$ as

$$E(r) = \sum_{j=1}^{N} U_j f_j(r)$$
$$f_j(r) = \begin{cases} 1/r, & r(j) < r < r(j+1) \\ 0, & r(j) > r > r(j+1) \end{cases} \tag{10}$$

where $r(j) = hj$, $h = L/N$ is "a step" on the line of matching the areas, L is the line section length of matching the areas, and N is the number of sections. Substituting (10) into (7), we come to the system of N linear equations in unknown coefficients U_j. The matrix elements in case of single discontinuity [see Fig. 1(a)] have the form

$$U_{kj} = \Big(\sqrt{\varepsilon_1}/\ln(b_1/a_1) + \sqrt{\varepsilon_2}/\ln(b_2/a_2)\Big) \ln(r_{k+1}/r_k) \cdot \ln(r_{j+1}/r_j) + ik_0 \cdot \Bigg\{\varepsilon_1 \sum_{n=1}^{N} 2.0 \Big/ \Big[\alpha_n \chi_n^2 \Big(b_1^2 Z_1^2(\chi_n b_1) - a_1^2 \cdot Z_1^2(\chi_n a_1)\Big)\Big] \cdot \Big[Z_0(\chi_n r_{k+1}) - Z_0(\chi_n r_k)\Big] \cdot \Big[Z_0(\chi_n r_{j+1}) - Z_0(\chi_n r_j)\Big] - \varepsilon_2 \sum_{m=1}^{M} 1.0 \Big/ \Big[\beta_m \kappa_m^2 b_2^2 Z_1^2(\kappa_m b_2) - a_2^2 Z_1^2(\kappa_m a_2))\Big] \cdot \Big[Z_0(\kappa_m r_{k+1}) - Z_0(\kappa_m r_k)\Big] \cdot \Big[Z_0(\kappa_m r_{j+1}) - Z_0(\kappa_m r_j)\Big]\Bigg\} - 2\sqrt{\varepsilon_1}\, \ln(r_{j+1}/r_j)$$

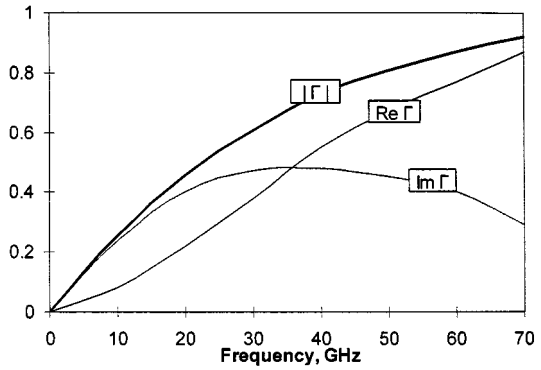

Fig. 2. Dependencies of the modulus, real, and imaginary parts of the reflection coefficient.

where N, M is a number of higher modes taken into account. The procedure described above actually results in matching by points the tangential components of the magnetic field at the planes of RCTLs' joints.

A package of programs for the analysis of single and interacting axially symmetrical stepped discontinuities in RCTLs has been developed on the basis of the method described above. The system of linear equations has been solved numerically with the application of the Gauss method, the main element being chosen by the columns.

The solution of test and real problems showed, in general, good convergence of the results under the increase of the section numbers N and M. This may be attributed to an appropriate choice of the system of basic functions (10), which allows one to take into consideration in an explicit form the basic propagating TEM mode. As an example of the computation with the method presented, Fig. 2 shows dependencies of the modulus, real, and imaginary parts of the reflection coefficient Γ_0 for the joints of RCTLs (the RCTL parameters [see Fig. 1(a)] are $b_1 = 3.5/2$ mm, $b_2 = 7/2$ mm, $a_1 = 1.52/2$ mm, $a_2 = 304/2$ mm, and $\varepsilon_1 = \varepsilon_2 = 1$).

To test the package, the parameters of the discontinuity shown in Fig. 1(a) have been computed. The comparison of the modeling results with those [3], [4] for the case $\varepsilon_1 = \varepsilon_2 = 1$ showed good convergence, as the discrepancy did not exceed 3%. It should be noted that the results of [3] and [4] have been obtained over a limited frequency range and with a small number of higher wave types considered.

IV. Optimization of 50-Ω Adapters for RCTLs

The discontinuity [see Fig. 1(b)] is most commonly used in practice as an element of wide-band matching of coaxial lines, which have different geometric dimensions and dielectric mediums. The first results of the theoretical analysis of such a discontinuity for an individual case of geometry have been obtained in [6]. In a quasi-static approach, it has been shown that for the case of 50-Ω RCTLs with air dielectric medium ($\varepsilon_1 = \varepsilon_2 = \varepsilon_3 = 1$), the prescription of the parameter d in the form

$$d = 2b_3 \ln\left(b_3/b_1\right) \Big/ \left(3.09 \times b_3/b_1\right) \tag{11}$$

is optimum. A more exact electrodynamics modeling has shown that the optimum values d_0 somewhat exceed those given by (11). However, the data published earlier is given in graphic form and is of illustrative character.

Let us solve the problem of the adapter optimization. Let us reduce it to the search of the value of the varied parameter vector $\mathbf{V}$ under which the reflection-coefficient module $|\Gamma|$ is minimum over the prescribed frequency range

$$\min_{\mathbf{V}} \max_{f \in [f_{\min}, f_{\max}]} |\Gamma(f, \mathbf{V})| \tag{12}$$

TABLE I
Optimization Results for a Coaxial-to-Coaxial Transmission-Line Adapter

b_3/b_1	$d_0/(2b_3)$	$d/(2b_3)$	$\mathrm{VSWR}_{0\max}$	$\mathrm{VSWR}_{\max}$
1.0	0.000	0.000	1.000	1.000
1.2	0.066	0.049	1.003	1.024
1.4	0.093	0.078	1.009	1.042
1.6	0.107	0.095	1.014	1.051
1.8	0.116	0.106	1.014	1.054
2.0	0.121	0.112	1.012	1.055
2.2	0.123	0.116	1.009	1.055
2.4	0.124	0.118	1.009	1.053
2.6	0.125	0.119	1.009	1.055
2.8	0.125	0.119	1.016	1.058
3.0	0.126	0.118	1.025	1.067
3.2	0.124	0.117	1.035	1.076
3.4	0.124	0.116	1.046	1.088
3.6	0.123	0.115	1.057	1.101
3.8	0.122	0.114	1.067	1.116
4.0	0.121	0.112	1.077	1.131
4.2	0.120	0.111	1.088	1.148

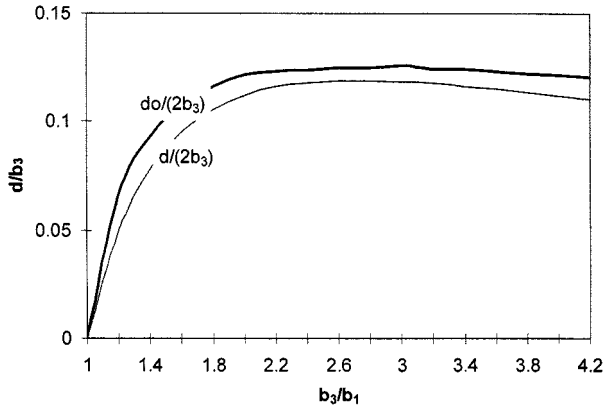

Fig. 3. d_0, d as functions of b_3/b_1.

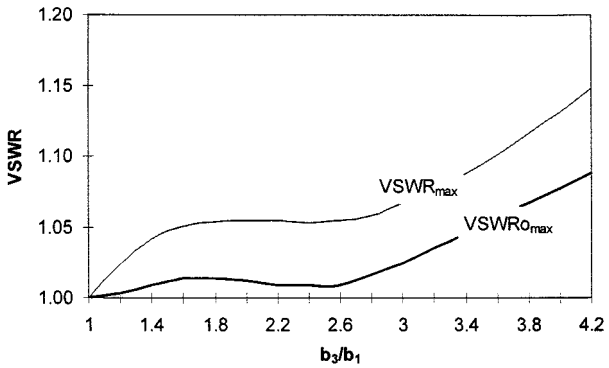

Fig. 4. $\mathrm{VSWR}_{0\ \max}$ and $\mathrm{VSWR}_{\max}$ as functions of b_3/b_1.

where $\mathbf{V} = (d)$ is the varied parameter vector. When solving the problem (12), we assumed that $b_1 = b_2$, $b_3 = 7/2$ mm, $a_1 = a_2$; $a_3 = 3.04/2$ mm, $\varepsilon_1 = \varepsilon_2 = \varepsilon_3 = 1$, $f_{\min} = 0$, and $f_{\max} = 20$ GHz.

Table I presents the results of the numerical optimization for the values $1 < b_3/b_1 < 4$. For convenience, Table I also presents the values of d computed according to (11), values of d_0, and the maximum values of the $\mathrm{VSWR}_{\max}$, and $\mathrm{VSWR}_{0\ \max}$ of the adapters, the lengths of matching sections of which are, respectively, d and d_0. Figs. 3 and 4 show plots of d, d_0, and also $\mathrm{VSWR}_{\max}$, $\mathrm{VSWR}_{0\ \max}$

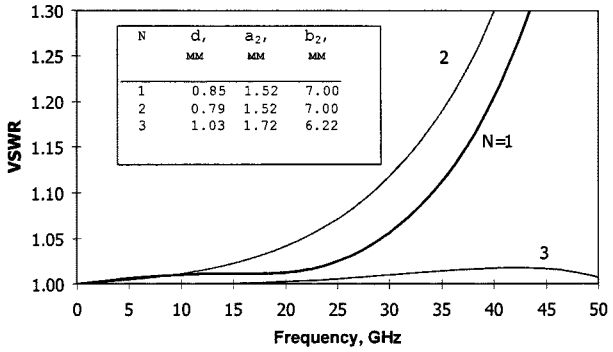

Fig. 5. Frequency characteristics of the adapters.

as functions of b_3/b_1. Fig. 5 (curves 1 and 2) shows frequency characteristics of the adapters for an RCTL, the lengths of the matching sections of which d_0, d correspond to the data given in Table I. The RCTL parameters [see Fig. 1(b)] are as follows: $a_1 = a_2 = 1.52/2$ mm, $a_3 = 3.04/2$ mm, $b_1 = 3.5/2$ mm, $b_2 = b_3 = 7/2$ mm, and $\varepsilon_1 = \varepsilon_2 = \varepsilon_3 = 1$.

In the research available, the solution of the adapter optimization problem was reduced to the choice of an optimum value d. It is obvious, however, that there exists the possibility of varying the geometrical dimensions of a_2, b_2 as well in the area of discontinuities. The numerical experiments carried out by the authors have shown that the variation of the geometrical dimensions of a_2, b_2 has a pronounced effect on the adapter frequency characteristics. In view of this, the optimization problems (12) have been solved in a new setup. It was assumed that $\mathbf{V} = (d, a_2, b_2)$, $f_{\max} = 50$ GHz. The results of the optimization problem solution are presented in Table II. Fig. 5 (curve 3) shows the plot of voltage standing wave ratio (VSWR) versus frequency for the connection of 50-Ω coaxial lines of 7.0/3.04 and 3.5/1.52 mm in cross sections over the frequency range from dc to 50 GHz. The geometrical dimensions of the matching element are shown in the table of Fig. 5.

Considerable practical advantages of the obtained solution of the optimization problem manifest themselves when the necessity arises to match RCTLs with large differences of geometrical dimensions. Such problems appear, e.g., while designing coaxial probes on RCTLs of particularly small cross sections. It is easy to verify that the use of the optimum solutions allows one to obtain satisfactory matching of the RCTLs, the geometrical dimension ratio of which reaches 8–12, with the help of only one discontinuity. When using the solutions corresponding to Table I, the solution of the analogous problem would require the use of a technically more complicated matching transformer of considerably greater length comprising from 2 to 4 discontinuities separated by the RCTL sections of a quarter-wavelength.

V. Experimental Results

In order to evaluate the reliability of the results obtained, the sample of the optimized adapter for an RCTL with increased geometric dimension ratio has been experimentally studied. The adapter design (Fig. 6) is formed by a compensating section with optimum geometrical dimensions 1 and volumetric absorber 2. The results of measuring the adapter return losses over the frequencies up to 50 GHz are given in Fig. 7 (curve 1). For comparison, the return losses' frequency characteristics (curve 2) of matched load on a volumetric absorber is also shown in this figure. The measurements were performed with the HP 8510 analyzer. It should be noted that rapid increase of return losses in the low-frequency region is motivated by the mismatching of volumetric absorbers. The results obtained testify to a good agreement of computed and experimental data.

TABLE II
Optimization Results for a Coaxial-to-Coaxial Transmission–Line Adapter

b_3/b_1	$d/(2b_3)$	a_2/b_3	b_2/b_3	$VSWR_{max}$
1.000	0.000	0.434	1.000	1.000
1.077	0.122	0.413	0.968	1.005
1.167	0.131	0.391	0.941	1.006
1.273	0.138	0.364	0.928	1.004
1.400	0.147	0.329	0.887	1.016
1.556	0.147	0.310	0.887	1.018
1.750	0.147	0.279	0.886	1.014
2.000	0.147	0.247	0.885	1.008
2.333	0.148	0.219	0.883	1.010
2.800	0.147	0.192	0.886	1.015
2.917	0.147	0.186	0.886	1.017
3.043	0.146	0.181	0.887	1.021
3.182	0.146	0.176	0.891	1.027
3.333	0.146	0.170	0.894	1.034
3.500	0.145	0.169	0.884	1.044
3.684	0.144	0.163	0.887	1.050
3.889	0.143	0.158	0.890	1.057
4.118	0.142	0.151	0.900	1.063
4.375	0.140	0.146	0.904	1.080
4.667	0.140	0.142	0.908	1.091
5.000	0.140	0.136	0.908	1.114
5.385	0.137	0.135	0.908	1.148
5.833	0.135	0.127	0.928	1.162
6.364	0.133	0.121	0.940	1.178
7.000	0.131	0.112	0.942	1.080
7.778	0.126	0.107	0.964	1.190
8.750	0.123	0.099	0.979	1.252
10.000	0.121	0.089	1.012	1.218
11.667	0.117	0.080	1.008	1.220

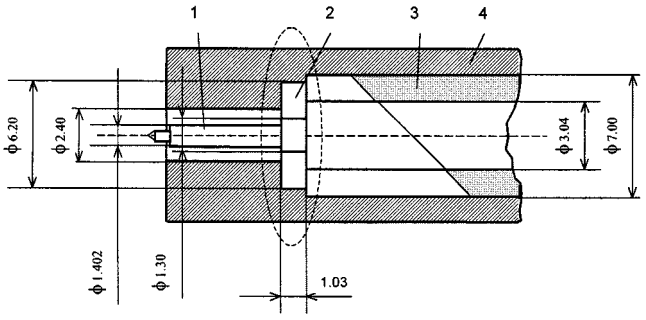

Fig. 6. Construction of the adapter. (1) Inner conductor of coaxial connector APC-2.4. (2) Matching element. (3) Volumetric absorber. (4) Body.

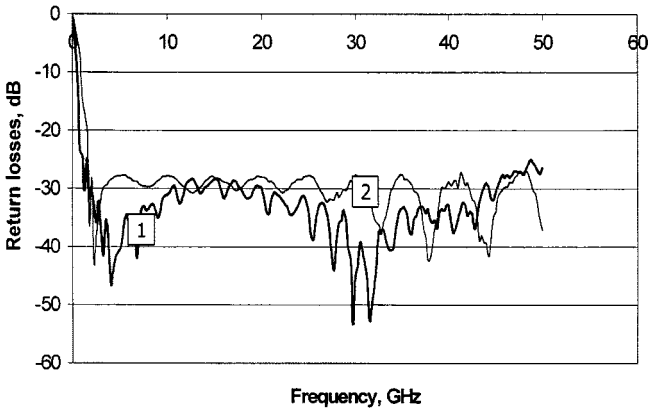

Fig. 7. Frequency characteristics. (1) Matched load on volumetric absorber HP00915-60004 (4.50 GHz). (2) Data of experiment.

VI. Summary

This paper has described an efficient algorithm for modeling axially symmetrical discontinuities in RCTLs suitable for the analysis of a wide class of axially symmetric nonuniformities with air and dielectric medium. On its basis, a package of programs for the synthesis of the devices on RCTLs has been developed. The solutions of the synthesis problems found provide a shortage of the adapter longitudinal dimensions and improve their electrical parameters for a wide range of geometrical dimensions. The results of the experimental research of the adapter for RCTLs of 2.4/1.042 mm in cross section to those of 7/3.04 mm over the frequency range from dc to 50 GHz have proven the reliability of the theoretical results obtained and the accuracy of the analysis and synthesis programs developed. The software created can be used for the development of various devices on RCTLs.

References

[1] J. R. Whinnery, H. W. Jamieson, and T. E. Robbins, "Coaxial line discontinuities," *Proc. IRE*, vol. 32, pp. 695–709, Nov. 1944.

[2] U. Shvinger, "Discontinuities in waveguides," *Zarubezhnaya radioelektron.*, no. 3–4, p. 106, 1970.

[3] P. I. Somlo, "Calculation of coaxial transmission line step capacitance," *IEEE Trans. Microwave Theory Tech*, vol. MTT-15, pp. 48–53, Jan. 1967.

[4] V. I. Volman and M. F. Maligin, "Exact electrodynamic analysis of the end stepped junction of coaxial waveguides," *Radiotekh.*, no. 4, pp. 65–68, 1988.

[5] T. E. Makkenzie and A. E. Sanderson, "Some fundamental design principles for the development of precision coaxial standards and components," *IEEE Trans. Microwave Theory Tech.*, vol. MTT-14, pp. 29–39, Jan. 1966.

[6] A. Krauss, "Measured curves of reflecting coefficients of compensated inhomogeneities in coaxial lines and the optimum dimensions deduced from them," *Rohde U. Schwarz Mitt*, vol. 8, pp. 1–12, Dec. 1956.